Electrocatalysis

International Edition: DOI: 10.1002/anie.201502836
German Edition: DOI: 10.1002/ange.201502836

CoOOH Nanosheets with High Mass Activity for Water Oxidation**

Junheng Huang, Junting Chen, Tao Yao, Jingfu He, Shan Jiang, Zhihu Sun, Qinghua Liu, Weiren Cheng, Fengchun Hu, Yong Jiang, Zhiyun Pan,* and Shiqiang Wei**

Abstract: *Endowing transition-metal oxide electrocatalysts with high water oxidation activity is greatly desired for production of clean and sustainable chemical fuels. Here, we present an atomically thin cobalt oxyhydroxide (γ-CoOOH) nanosheet as an efficient electrocatalyst for water oxidation. The 1.4 nm thick γ-CoOOH nanosheet electrocatalyst can effectively oxidize water with extraordinarily large mass activities of 66.6 $A g^{-1}$, 20 times higher than that of γ-CoOOH bulk and 2.4 times higher than that of the benchmarking IrO_2 electrocatalyst. Experimental characterizations and first-principles calculations provide solid evidence to the half-metallic nature of the as-prepared nanosheets with local structure distortion of the surface CoO_{6-x} octahedron. This greatly enhances the electrophilicity of H_2O and facilitates the interfacial electron transfer between Co ions and adsorbed -OOH species to form O_2, resulting in the high electrocatalytic activity of layered CoOOH for water oxidation.*

Water splitting assisted by electricity or sunlight has been regarded as a promising way to provide clean and sustainable energy source of hydrogen for powering fuel cells and reducing CO_2 to fuels.[1] In the process of water splitting, the oxidative half reaction of oxygen evolution reaction (OER) is kinetically sluggish and requires large overpotentials and the use of electrocatalyst.[2] For this reason, a number of electrocatalysts have been explored to lower the overpotential and accelerate the OER reaction, and thereby enhance the energy conversion efficiency.[3] It is known that the most active OER electrocatalysts are IrO_2 or RuO_2, but their scarcity and high cost limit the large-scale application.[4] Therefore, it is highly desirable yet challenging to develop an active and earth-abundant OER catalyst for the water oxidation reaction.

[*] J. H. Huang,[+] J. T. Chen,[+] Dr. T. Yao, Dr. J. F. He, S. Jiang, Dr. Z. H. Sun, Dr. Q. H. Liu, W. R. Cheng, F. C. Hu, Dr. Y. Jiang, Dr. Z. Y. Pan, Prof. S. Q. Wei
National Synchrotron Radiation Laboratory
University of Science and Technology of China
Hefei 230029 (P.R. China)
E-mail: qhliu@ustc.edu.cn
zhypan@ustc.edu.cn
sqwei@ustc.edu.cn

[+] These authors contributed equally to this work.

[**] This work was supported by the National Natural Science Foundation of China (grants no. 11135008, 11435012, U1332111, 11305174, 11422547, 11205158, and 21471143), the National Basic Research Program of China (2012CB825800), and the Foundation for Innovative Research Groups of the National Natural Science Foundation of China (11321503). We thank NSRL, BSRF, and SSRF for synchrotron beamtime.

Supporting information for this article is available on the WWW under http://dx.doi.org/10.1002/anie.201502836.

Transition metal oxides (TMOs) and their derivatives are attractive electrocatalyst candidates due to their diversity and potential stability.[5] Among the TMOs systems, according to the "volcano" relation model,[3b] cobalt-based oxides show high promise as good water oxidation catalysts. For example, Co-phosphate compounds have been reported efficiently working and self-healing in neutral and weakly basic medium.[6] Co- or Ni-based layered hydroxides or oxyhydroxides are found to exhibit enhanced water oxidation activity in alkaline medium.[7] However, catalytic efficiencies of these materials are still below what is expected, with higher overpotential (0.35–0.4 V) and lower water oxidation performance than IrO_2. The underperformance is mainly ascribed to the fully occupied bonding t_{2g} orbitals of MO_6 center that induces a low electron transfer conductivity and impedes the reaction of an OH^- anion with an adsorbed O atom on the catalytic active sites to form adsorbed -OOH species. As a result, a critical rate-limiting step in the process of water splitting is formed, which apparently increases the water oxidation reaction barrier and decreases the mass activity in water oxidation reaction. Therefore, it is highly desirable to develop a new strategy to overcome these disadvantages for achieving excellent electrocatalytic activity of this kind of promising compounds. Recently, two-dimensional (2D) ultrathin nanosheets have attracted tremendous attention because of their fascinating physical and chemical properties induced by the dimensional confinement.[8] In the nanosheets with few-layer thickness, nearly all the metal ions are exposed that can tune the band gap states and increase the density of states near the Fermi level. Hence, these exposed metal ions can serve as highly active sites for catalytic reactions,[9] beneficial for fast interfacial charge transfer and facile electrochemical reactions to decrease the catalytic reaction barrier.[10] Therefore, 2D ultrathin nanosheets with atomic thickness are eagerly anticipated to be able to tune OER activity of metal hydroxides or oxyhydroxides.

In this work, taking an "atomic-scale phase transformation" strategy, we have synthesized ultrathin γ-CoOOH nanosheets that show half-metallic behavior and possess significantly reduced apparent activation energy of 26 meV. Our synthetic strategy is facile and performed at room temperature. The obtained few-atomic-layered γ-CoOOH nanosheet can effectively catalyze water oxidation with an extremely large mass activity of 66.6 $A g^{-1}$ at a quite small overpotential of 0.30 V, 20 times higher than that of bulk counterpart and also higher than that of the state-of-the-art IrO_2 electrocatalyst. The as-synthesized nanosheets are characterized by low OER overpotential of 0.30 V at 10 $mA cm^{-2}$, low Tafel slope of 38 mV/dec, large turnover frequencies (TOFs) of 0.09 s^{-1} and long operation stability in alkaline environment. The dimensional confinement in ultra-

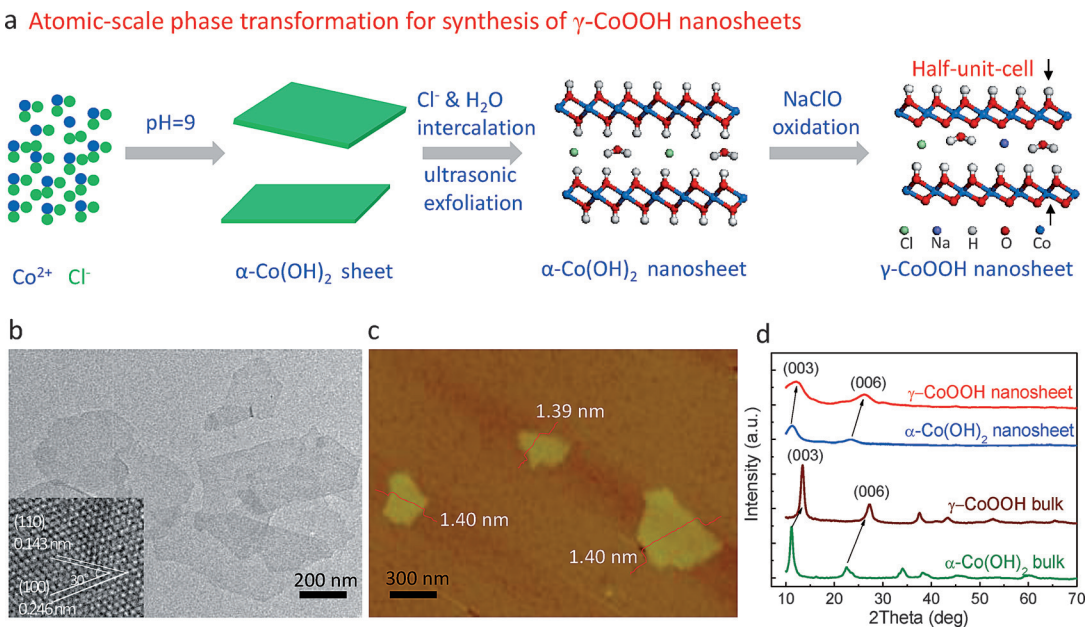

Figure 1. a) Synthetic route for the γ-CoOOH nanosheets. b) TEM image and c) AFM image for the γ-CoOOH nanosheets. The inset in (b) shows the HRTEM image for the γ-CoOOH nanosheets. d) XRD pattern for the γ-CoOOH nanosheets. The patterns of bulk γ-CoOOH and bulk and nanosheet α-$Co(OH)_2$ are also displayed for comparison.

thin nanosheet can largely modify the electronic structure of the material and facilitate the electron transfer and conversion in the CoO_{6-x} octahedron of the nanosheet surface. Our γ-CoOOH nanosheets results provide prospective insights into the design of high performance electrocatalysts for water oxidation electrocatalysis.

Based on the fact that α-$Co(OH)_2$ and γ-CoOOH have similar spatial structure but different interslab spacing, we designed a two-step soft chemistry route of "atomic-scale phase transformation process" to synthesize γ-CoOOH nanosheets for the first time (Figure 1a and Supporting Information (SI)). First, layered α-$Co(OH)_2$ sheets were prepared by a facile wet chemistry method.[11] The obtained α-$Co(OH)_2$ was then sonicated into ultrathin nanosheets via liquid exfoliation in the presence of Cl^- anions and water that can enlarge the interlayer distance. Then, the α-$Co(OH)_2$ nanosheets with large interlayer spacing were dehydrogenated and transformed to γ-CoOOH nanosheets by NaClO oxidant at room temperature. The formation of ultrathin nanosheets was demonstrated by the colloidal nature of the solution (Tyndall effect in Figure S1 in the SI). Further, the ultrathin nanosheets can be directly observed by transmission electron microscopy (TEM) image in Figure 1b, which have a faint contrast, verifying their very thin nature. Atomic force microscopy (AFM) image shows clearly that nanosheets are several hundred nanometers in size with thickness of about 1.4 nm, corresponding to the half-unit-cell height of a γ-CoOOH cell along the *c*-axial direction. X-ray diffraction pattern (XRD) in Figure 1d reveals that the γ-CoOOH ultrathin nanosheet possesses a highly (00*n*) preferred orientation, and it is further verified by their corresponding high-resolution TEM (HRTEM) image (inset of Figure 1b). Therefore, all above results clearly demonstrate that ultrathin γ-CoOOH nanosheets were successfully fabricated.

To determine the electronic property of the ultrathin γ-CoOOH nanosheet, temperature-dependent electrical conductivity was measured (Figure S4). Figure 2a shows the linear relationship between the logarithm of the conductivity with respect to the reciprocal of the temperature in the Arrhenius plot. We find that the conductivity of ultrathin γ-CoOOH nanosheet is $4.4\times10^{-1}\,S\,cm^{-1}$ at room temperature (Figure 2a and Figure S4), about 52 times higher than the $8.5\times10^{-3}\,S\,cm^{-1}$ of bulk counterpart, manifesting a half-metallic character of the ultrathin γ-CoOOH nanosheets.[12] This can be further confirmed by the electrochemical impedance characterization shown in Figure 2b, which reveals a decreased transport resistance of γ-CoOOH nanosheets (inset of Figure 2b). The apparent activation energy (E_a) is also an important electronic property influencing the water oxidation catalytic activity. The E_a of each sample can be derived from the slope of the fitting straight lines in Figure 2a (see section S6 in the SI). As a result of emerging half-metallic state, the E_a of γ-CoOOH nanosheet is as low as 26 meV, compared to 154 meV for the bulk counterpart. It should also be noted that the E_a value of our γ-CoOOH nanosheet is much lower than those of other transition-metal oxide nanosheets, such as 50–300 mV for Fe_2O_3 and Co_3O_4 nanosheets.[8c] This drastically decreased E_a would greatly accelerate the exchange of carriers in the ultrathin nanosheet relative to the bulk γ-CoOOH, which is critical for the surface catalytic reaction. These results demonstrate that the electronic properties of γ-CoOOH nanosheets are strongly improved for the catalytic water oxidation reaction.

The water oxidation activities of the ultrathin γ-CoOOH nanosheets were evaluated by steady-state electrochemistry measurements in 1M KOH solutions using a typical three-electrode cell setup (see details in the SI). As shown in Figure 2c, the polarization curve recorded with the γ-

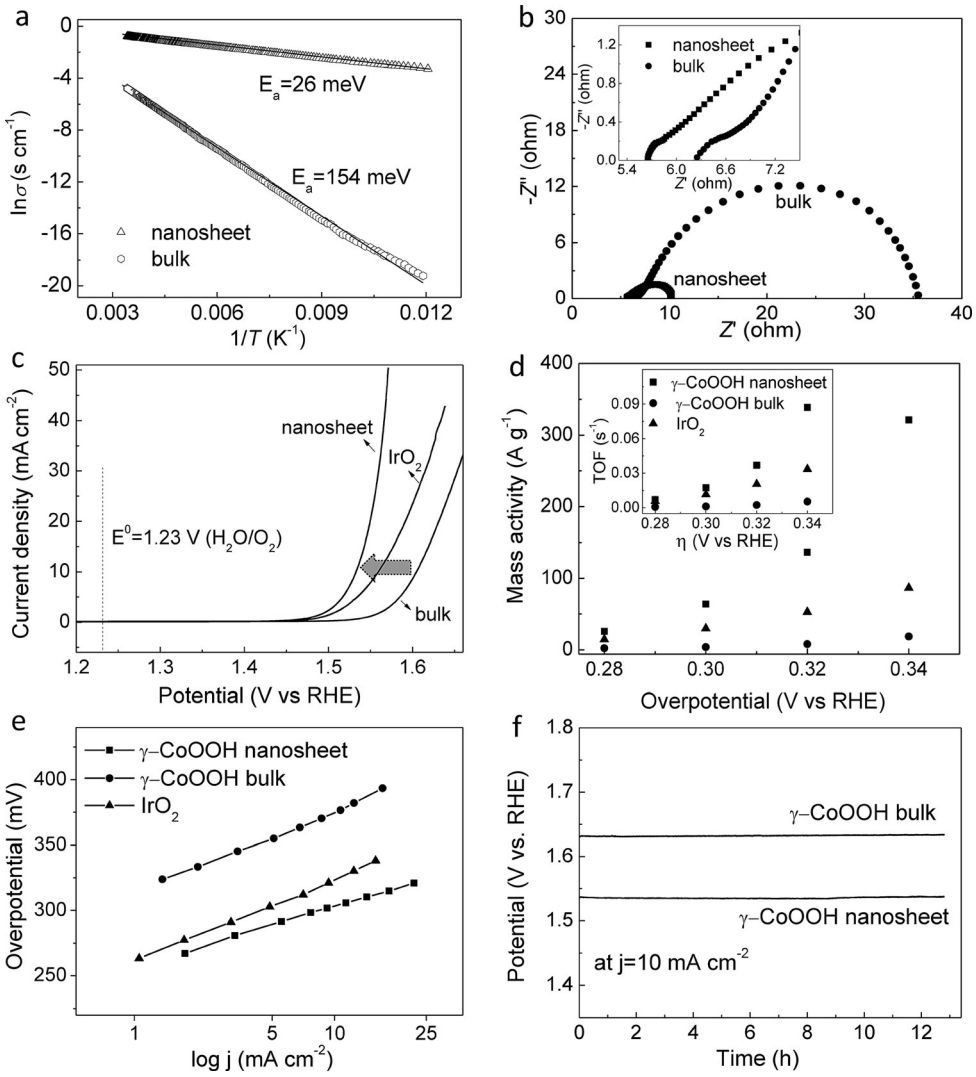

Figure 2. a) Temperature-dependent conductivity plots and b) electrochemical impedance spectra of ultrathin γ-CoOOH nanosheets and bulk γ-CoOOH. c) Polarization curves, d) mass activities, and e) Tafel plots in 1 M KOH medium with ultrathin γ-CoOOH nanosheets, bulk γ-CoOOH, and IrO_2 as the electrocatalysts. The TOFs for ultrathin γ-CoOOH nanosheets, bulk γ-CoOOH, and IrO_2 at different overpotentials are shown in inset of (d). f) Chronopotentiometric measurements at $J = 10\ mA\,cm^{-2}$ for bulk and nanosheet γ-CoOOH.

CoOOH nanosheets reveals a markedly small onset potential of 1.47 V for the OER, beyond which the anodic current rises fast by applying a smaller overpotential (from 2.3 $mA\,cm^{-2}$ at 1.50 V to 50 $mA\,cm^{-2}$ at 1.58 V). In contrast, bulk γ-CoOOH shows an inferior OER activity with a larger onset potential of 1.53 V (Figure 2c) and slower current increase (ca. 1.2 $mA\,cm^{-2}$ at 1.56 V). It needs to be specially noted that the mass activity of γ-CoOOH nanosheets is 66.6 $A\,g^{-1}$ at a quite small overpotential of 0.3 V, which is ca. 20 times higher than bulk γ-CoOOH and twice that of the state-of-the-art IrO_2 electrocatalyst (see Figure 2d and Table 1). To the best of our knowledge, the mass activities for our γ-CoOOH nanosheet is the highest among the reported OER catalysts.[10] The enhanced catalytic activity of the γ-CoOOH nanosheet is also reflected by its low Tafel slope of 38 mV/dec (Figure 2e), leading to an even higher enhancement in OER activity at $\eta > 300$ mV. Although the onset potentials of γ-CoOOH nanosheets and IrO_2 catalyst are similar (1.47 V vs 1.48 V), the overpotential (330 mV at 10 $mA\,cm^{-2}$) and Tafel slope (52 mV/dec) for IrO_2 are evidently higher than those of γ-CoOOH nanosheets (Table 1). The γ-CoOOH nanosheet also exhibits a linear increase in TOF with overpotential, affording much higher TOFs than bulk γ-CoOOH and IrO_2 (inset of Figure 2d). The above results demonstrate that ultrathin γ-CoOOH nanosheet has an excellent catalytic water oxidation activity, remarkably outperforming the precious IrO_2 electrocatalyst.

The long-term performance and stability is another significant criterion to evaluate an electrocatalyst especially for commercial applications. To assess the durability of the ultrathin γ-CoOOH nanosheets in an alkaline environment, continuous potential cycling at a constant current density J of 10 $mA\,cm^{-2}$ was performed in O_2-saturated 1 M KOH solution for 13 h. Figure 2f shows that γ-CoOOH nanosheets have good electrochemical stability, as the overpotential remained almost constant during 13 h. Of note, the overpotential of bulk γ-CoOOH was also nearly constant during the 13 h operation, suggesting a strong intrinsic OER stability of the γ-CoOOH material. However, the overpotential for maintaining a J of 10 $mA\,cm^{-2}$ for IrO_2 increased from 335 to 402 mV during 5 h (Figure S5), which is basically consistent with the reported results.[4,7a] Moreover, the polarization curve of γ-

Table 1: Comparison of OER activities for various samples in alkaline medium.

Catalyst	Onset potential (V vs. RHE)	η at 10 $mA\,cm^{-2}$ [mV]	Mass activity at $\eta = 0.30$ V [$A\,g^{-1}$]	Tafel slope [mV/dec]
γ-CoOOH NS[a]	1.47	300	66.6	38
γ-CoOOH bulk	1.53	374	3.4	55
IrO_2	1.48	330	27.5	52

[a] NS = nanosheets.

CoOOH nanosheets after 1000 cycles (see Figure S6a) almost overlaid the *J–V* curve of the first cycle, with only negligible drops of the anodic current. The ultrathin nanosheets also possess a high structural stability during the catalytic reaction. The XRD patterns of the nanosheets (Figure S6b) display no apparent variations after the electrocatalytic reaction. Therefore, all above results indicate that ultrathin γ-CoOOH nanosheets possess superior electrocatalytic activity as well as structural stability in a long-term electrochemical process.

To give an in-depth understanding of the high water oxidation activity of the γ-CoOOH nanosheets, X-ray absorption fine structure spectroscopy (XAFS) was performed. As shown in Figure 3a, the Co K-edge extended XAFS (EXAFS) $k^3\chi(k)$ oscillation curve for the ultrathin nanosheet displays a noticeable difference in 2–8 $Å^{-1}$ in comparison with the bulk material, implying the different cobalt local atomic arrangements. Moreover, the Fourier transforms (FTs) curves of bulk and nanosheet γ-CoOOH are characterized by two main peaks at 1.48 Å and 2.50 Å (Figure 3b), corresponding to the nearest Co–O and next nearest Co–Co coordinations, respectively. Strikingly, these peak intensities of the γ-CoOOH nanosheet show significant decrease. The Co–O coordination number decreased from 6.0 for the bulk to 5.1 for nanosheet (Table S2), suggesting that the ultrathin nature of the nanosheet resulted in the presence of a large amount of dangling bonds in the surface Co octahedron (CoO_{6-x}) with a structural distortion. Correspondingly, the electronic structure for ultrathin nanosheet is changed by the local structural distortion of CoO_{6-x} octahedrons. As shown in the X-ray absorption near-edge spectra (XANES) (Figure 3c), the absorption edge of ultrathin γ-CoOOH nanosheet shifted 1.3 eV towards lower energy relative to that of bulk, corresponding to a change in the Co valence state from +3.2 for the bulk to +2.8 for nanosheet γ-CoOOH.[13] The variation of electronic state can be further confirmed by the X-ray photoelectron spectroscopy (XPS) result (Figure 3d), which shows the emergence of a shake-up shoulder at the higher energy side of the Co 2p signal for γ-CoOOH nanosheets.

To clarify the influence of atomic and electronic structure variation on the OER activity, we performed first-principles energy and band structure calculations based on the structure model from the XAFS results. Evidently, the density of states (DOS) around the Fermi level for γ-CoOOH nanosheet is quite different from that of bulk (Figure 4a). Because of the two-dimensional confinement effect, the Fermi level crosses the spin-up states while within the band gap of the spin-down states of γ-CoOOH nanosheet (upper panel of Figure 4a), demonstrating a typical half-metallic character as confirmed by previous electrical measurements. The surface structural distortion of the CoO_{6-x} octahedron as evidenced by EXAFS results could break the degeneracy of hexagonal Co arrangement in γ-CoOOH nanosheet.[8c] Correspondingly, the degeneracy breaking of Co ions rearranges the Co 3d electrons population with the appearance of partially occupied antibonding e_g orbitals along with the unoccupied t_{2g} states, resulting in the formation of $t_{2g}^5e_g^{1.2}$ configuration. This can be confirmed by the Co 2p XPS result, which shows a shake-up shoulder at the higher energy side. These electronic characteristics have several advantages in improving OER catalytic performance of γ-CoOOH nanosheet. First, the increased hole states in the t_{2g} orbital of CoO_{6-x} can enhance the electrophilicity of the adsorbed O, and facilitate the adsorption of the hydroxy group on the catalytically active sites to form adsorbed -OOH species (Figure 4b).[14] Second, because the σ-bonding e_g orbital has a stronger ability to overlap with the oxygen-related adsorbate than the π-bonding t_{2g} orbital, it can promote electron transfer between surface cation (CoO_{6-x}) and adsorbed -OOH intermediates more directly.[4] Figure 4c compares the calculated binding energy of H_2O molecules on

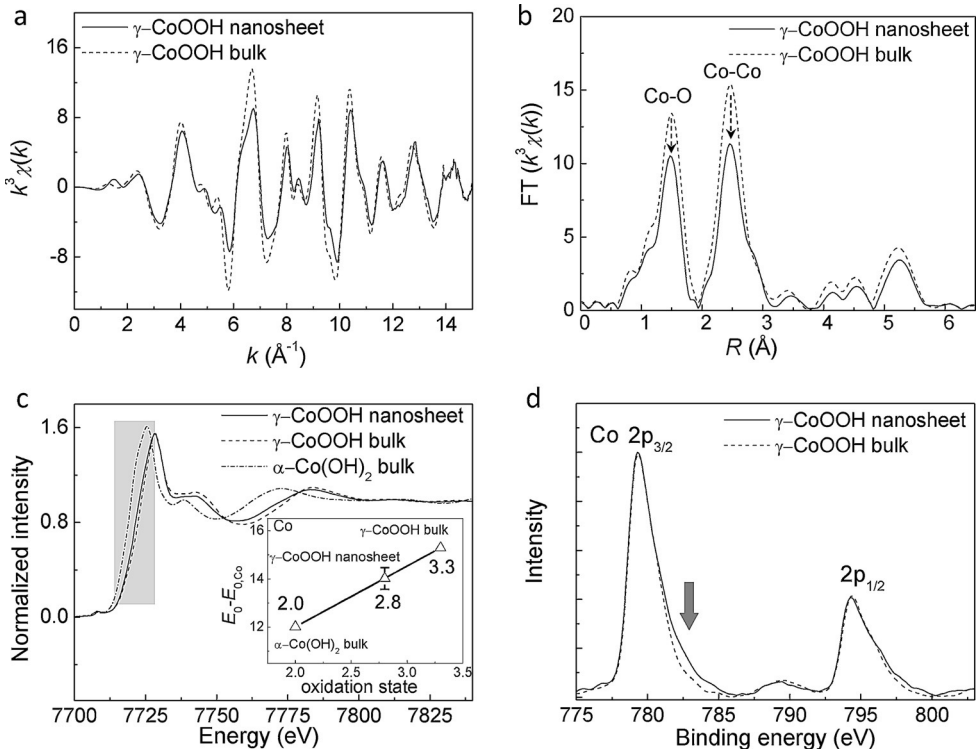

Figure 3. a) Co K-edge EXAFS $k^3\chi(k)$ oscillation functions and b) the corresponding FT curves of ultrathin γ-CoOOH nanosheets and bulk γ-CoOOH. c) XANES spectra for nanosheet and bulk γ-CoOOH and bulk α-Co(OH)$_2$ (inset: fitted oxidation states of Co). d) XPS spectra for Co of nanosheet and bulk γ-CoOOH.

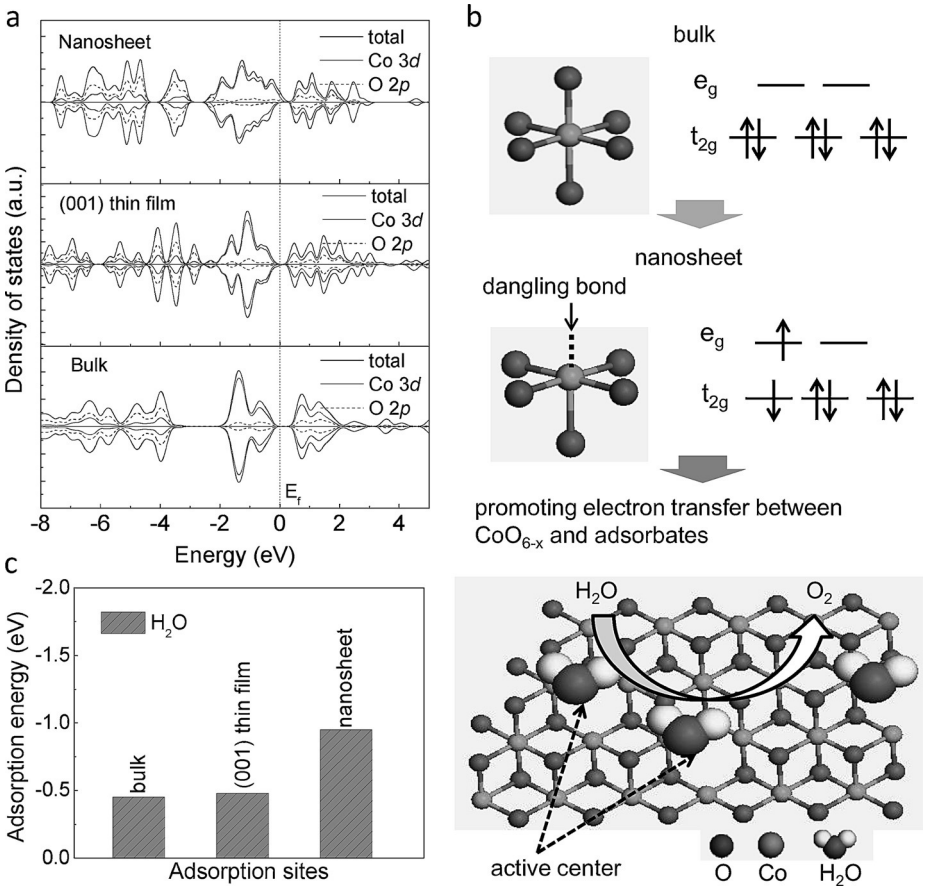

Figure 4. a) Calculated density of states (DOS) for γ-CoOOH nanosheet, γ-CoOOH (001) thin film and bulk γ-CoOOH. b) Electronic structure transformation of ultrathin γ-CoOOH nanosheet and model of water oxidation on the nanosheet surface. c) Calculated adsorption energy for ultrathin γ-CoOOH nanosheet, γ-CoOOH (001) thin film and bulk γ-CoOOH.

various cobalt sites. It is clear that the surface cobalt sites in the CoO_{6-x} octahedron possess adsorption energy of 0.95 eV (absolute value), obviously larger than that of CoO_6 in nanosheet (0.72 eV) and bulk γ-CoOOH (0.45 eV). This indicates that the surface CoO_{6-x} with structural distortion are more favorable for adsorbing H_2O molecules, playing a crucial role in the water oxidation activity. Consequently, the water oxidation barrier can be decreased and a much smaller OER overpotential is achieved.[4,15] It should be mentioned that the calculated DOS around the Fermi level for a 5 nm γ-CoOOH (001) thin film with similar surface structure to that of nanosheet shows no evident difference, in comparison with that of bulk γ-CoOOH (Figure 4a). Also, the adsorption energy of H_2O molecule on γ-CoOOH (001) thin film shows no evident improvement and is similar to that of bulk γ-CoOOH (Figure 4c). These results consolidate that the improved OER activity is mainly attributed to the two-dimension confinement in the γ-CoOOH nanosheet with a lower apparent activation energy of 26 meV, and the large surface area of the nanosheet increases the number of active centers for the OER reaction.

In summary, we have reported for the first time an ultrathin γ-CoOOH nanosheet as an efficient electrocatalyst for water oxidation, via a two-dimensional "atomic-scale phase transformation" strategy. Our developed γ-CoOOH nanosheets with atomically-layered thickness can change the electronic structure to half-metallic behavior. Their electric conductivity is increased by ca. 52 times in comparison to that of the bulk, and the apparent activation energy is reduced to as low as 26 meV. Benefiting from enhanced electrical conductivity with half-metallic behavior, the γ-CoOOH nanosheets realize impressive performance for water oxidation reaction with large mass activity of 66.6 $A\,g^{-1}$, low overpotential of 0.30 V, small Tafel slopes of 38 mV/dec and great durability in alkaline medium, which are superior to its bulk counterparts, commercial IrO_2, and the best known TMO electrocatalysts. The insights gained from XAFS and first-principles calculations provide clear evidence for the presence of the coordination-unsaturated CoO_{6-x} octahedrons that can change the valence electron configuration of Co 3d states and thus serve as active sites to effectively adsorb H_2O molecules and decrease the OER barrier, resulting in the significantly improved water oxidation performance. These results not only suggest the promise of an efficient, robust, and economic water oxidation electrocatalyst based on ultrathin γ-CoOOH nanosheets, but also open an avenue into the design of highly active and stable electrocatalysts towards global scale clean energy production.

Keywords: electrocatalysis · half-metallic · water oxidation · XAFS · γ-CoOOH nanosheets

How to cite: *Angew. Chem. Int. Ed.* **2015**, *54*, 8722–8727
Angew. Chem. **2015**, *127*, 8846–8851

[1] a) N. S. Lewis, D. G. Nocera, *Proc. Natl. Acad. Sci. USA* **2006**, *103*, 15729–15735; b) J. Liu, Y. Liu, N. Liu, Y. Han, X. Zhang, H. Huang, Y. Lifshitz, S. T. Lee, J. Zhong, Z. Kang, *Science* **2015**, *347*, 970–974; c) M. Guo, K. Y. Xie, J. Lin, Z. H. Yong, C. T. Yip, L. M. Zhou, Y. Wang, H. T. Huang, *Energy Environ. Sci.* **2012**, *5*, 9881–9888.

[2] M. T. M. Koper, *J. Electroanal. Chem.* **2011**, *660*, 254–260.

[3] a) R. K. Hocking, R. Brimblecombe, L. Y. Chang, A. Singh, M. H. Cheah, C. Glover, W. H. Casey, L. Spiccia, *Nat. Chem.* **2011**, *3*, 461–466; b) M. G. Walter, E. L. Warren, J. R. McKone, S. W. Boettcher, Q. X. Mi, E. A. Santori, N. S. Lewis, *Chem. Rev.* **2010**, *110*, 6446–6473.

[4] J. Suntivich, K. J. May, H. A. Gasteiger, J. B. Goodenough, Y. Shao-Horn, *Science* **2011**, *334*, 1383–1385.

[5] a) R. D. L. Smith, M. S. Prevot, R. D. Fagan, Z. P. Zhang, P. A. Sedach, M. K. J. Siu, S. Trudel, C. P. Berlinguette, *Science* **2013**, *340*, 60 – 63; b) M. W. Louie, A. T. Bell, *J. Am. Chem. Soc.* **2013**, *135*, 12329 – 12337; c) L. Trotochaud, J. K. Ranney, K. N. Williams, S. W. Boettcher, *J. Am. Chem. Soc.* **2012**, *134*, 17253 – 17261; d) C. Z. Yuan, H. B. Wu, Y. Xie, X. W. Lou, *Angew. Chem. Int. Ed.* **2014**, *53*, 1488 – 1504; *Angew. Chem.* **2014**, *126*, 1512 – 1530.

[6] M. W. Kanan, D. G. Nocera, *Science* **2008**, *321*, 1072 – 1075.

[7] a) F. Song, X. L. Hu, *Nat. Commun.* **2014**, *5*, 4477; b) R. Subbaraman, D. Tripkovic, K. C. Chang, D. Strmcnik, A. P. Paulikas, P. Hirunsit, M. Chan, J. Greeley, V. Stamenkovic, N. M. Markovic, *Nat. Mater.* **2012**, *11*, 550 – 557.

[8] a) A. K. Geim, *Science* **2009**, *324*, 1530 – 1534; b) F. Schwierz, *Nat. Nanotechnol.* **2010**, *5*, 487 – 496; c) W. R. Cheng, J. F. He, T. Yao, Z. H. Sun, Y. Jiang, Q. H. Liu, S. Jiang, F. C. Hu, Z. Xie, B. He, W. S. Yan, S. Q. Wei, *J. Am. Chem. Soc.* **2014**, *136*, 10393 – 10398; d) Y. F. Sun, Q. H. Liu, S. Gao, H. Cheng, F. C. Lei, Z. H. Sun, Y. Jiang, H. B. Su, S. Q. Wei, Y. Xie, *Nat. Commun.* **2013**, *4*, 2899; e) P. Xiong, B. R. Liu, V. Teran, Y. Zhao, L. L. Peng, X. Wang, G. H. Yu, *ACS Nano* **2014**, *8*, 8610 – 8616.

[9] D. Voiry, H. Yamaguchi, J. W. Li, R. Silva, D. C. B. Alves, T. Fujita, M. W. Chen, T. Asefa, V. B. Shenoy, G. Eda, M. Chhowalla, *Nat. Mater.* **2013**, *12*, 850 – 855.

[10] Y. F. Sun, Z. H. Sun, S. Gao, H. Cheng, Q. H. Liu, J. Y. Piao, T. Yao, C. Z. Wu, S. L. Hu, S. Q. Wei, Y. Xie, *Nat. Commun.* **2012**, *3*, 1057.

[11] J. B. Zhu, L. F. Bai, Y. F. Sun, X. D. Zhang, Q. Y. Li, B. X. Cao, W. S. Yan, Y. Xie, *Nanoscale* **2013**, *5*, 5241 – 5246.

[12] G. Eda, C. Mattevi, H. Yamaguchi, H. Kim, M. Chhowalla, *J. Phys. Chem. C* **2009**, *113*, 15768 – 15771.

[13] F. Bardé, M. R. Palacin, Y. Chabre, O. Isnard, J. M. Tarascon, *Chem. Mater.* **2004**, *16*, 3936 – 3948.

[14] Z. Y. Lu, H. T. Wang, D. S. Kong, K. Yan, P. C. Hsu, G. Y. Zheng, H. B. Yao, Z. Liang, X. M. Sun, Y. Cui, *Nat. Commun.* **2014**, *5*, 4345.

[15] X. N. Dang, H. J. Yi, M. H. Ham, J. F. Qi, D. S. Yun, R. Ladewski, M. S. Strano, P. T. Hammond, A. M. Belcher, *Nat. Nanotechnol.* **2011**, *6*, 377 – 384.

Received: March 27, 2015
Revised: April 22, 2015
Published online: June 10, 2015

